Critical Behavior in Quenched Random Structures: Mean-Field Lattice-Gas Approach

S. De and Y. Shapir
Dept. of Physics and Astronomy, University of Rochester, Rochester, NY 14627

E. H. Chimowitz and V. Kumaran
Dept. of Chemical Engineering, University of Rochester, Rochester, NY 14627

A new mean-field equation-of-state model is proposed for predicting the critical behavior of fluids confined in porous, random structures. The approach is based on a lattice-gas formalism and incorporates effects of both fluid confinement and energetically heterogeneous interactions between fluid molecules and pore surfaces. The model was used to predict a variety of thermodynamic properties in these systems, including the dependence of the confined fluid's critical properties on the porosity and relative strength of fluid–fluid and fluid–pore interaction energies. The study of surface-energy heterogeneities show that they significantly affect the critical temperature of the confined fluid, at a given porosity, compared to the uniform energy case. Comparison of the model performance with both grand canonical Monte Carlo simulation results and a set of adsorption data in a silica gel suggest that the approach taken here provides a useful analytic method for calculating physical properties in complex systems of this kind.

Introduction

The prediction of properties in complex materials is a problem of importance in many applications in chemical and materials engineering; by the term "complex material" we mean a heterogeneous substance like a porous material containing a confined fluid. Such materials appear in many technological applications, including (1) processes using supercritical fluids to dry porous aerogels and thin films (Rangarajan and Lira, 1991; VonBehren et al., 1997), (2) physical adsorption of trace components from gaseous effluents (Jing et al., 1994; Tapia-Corzo et al., 1999), (3) gas storage using microporous materials (Tan and Gubbins, 1990; Cracknell et al., 1993; Wang and Johnson, 1999a,b), and (4) chemical separations using inorganic membranes (Afrane and Chimowitz, 1996). Inorganic membranes are often highly porous, randomly structured materials with large surface areas available for adsorption, a property that makes them useful in chemical separations and as catalyst supports. In addition to their heterogeneity, complex materials have another distinguishing characteristic that relates to the structure of the heterogeneity itself. Is it periodic or dispersed throughout in some random fashion? These two situations are quite distinct and may, in each instance, show critical behavior for a confined fluid belonging to entirely different universality classes (Wong and Chan, 1990). In this article we investigate the critical properties of fluids confined in randomly structured host materials, like that found in porous silicon (VonBehren et al., 1997).

There is an extensive literature devoted to studying adsorption phenomena in disordered porous systems. Most prior theoretical work has utilized computer simulation (Kaminsky and Monson, 1991, 1994; Patrykiejew, 1993; Gac et al., 1996; MacFarland et al., 1996), integral equation theory (Madden and Glandt, 1988; Fanti et al., 1990; Kierlik et al., 1998), density functional methods (Tarazona, 1985; Evans et al., 1986; Evans, 1990), and/or combinations thereof (Ayappa et al., 1999) to study these systems. There have been very few papers, however, devoted specifically to the question of critical behavior in these systems. When this topic has been addressed, confined fluid systems have usually been viewed as experimental realizations of either the Random Field Ising Model (RFIM) or one of its closely associated models (De-Gennes, 1984; Imry and Ma, 1975). The RFIM is an Ising

Correspondence concerning this article should be addressed to E. H. Chimowitz.

spin system with each spin subjected to a local random field with a given symmetric distribution uncorrelated with the random fields on the other spins. Variants of this model have included the RFIM with nonsymmetric field distributions (Maritan et al., 1991), and the site-diluted RFIM (SD-RFIM), where the system is made dilute by removing spins from the lattice (Fishman and Aharony, 1979). These particular approaches, however, neglect the effects of confinement on the fluid, as discussed by Kierlik et al. (1998), and their use of analyzing confined fluid systems, accounting for the effects of both confinement and the relative strengths of fluid–fluid and fluid–surface interactions, is still an open issue that is taken up here.

Fortunately, there have been several experimental articles published in this area with which to guide and evaluate theoretical work. Findenegg and coworkers presented experimental adsorption data for a bulk, near-critical fluid adsorbing onto a plane solid surface (Specovius and Findenegg, 1978, 1980; Findenegg and Specovius, 1980; Findenegg and Loring, 1984). Blumel and Findenegg (1985) measured the scaling exponent of the surface excess adsorption of SF_6 on plane graphitized carbon and found a value that was at variance with theoretical predictions for this property, a result they attributed to confined geometry and/or nonasymptotic scaling effects.

Phase transitions of fluids in random porous structures like aerogels (Goh et al., 1987; Wong and Chan, 1990; Wong et al., 1993) and glasses (Thommes and Findenegg, 1994, 1995) have also been experimentally studied. Thommes and Findenegg (1994) studied the phase behavior of SF_6 confined in a controlled pore-size glass with a narrow pore-size distribution. They provided, to our best knowledge, the first data for the capillary condensation line up to the pore fluid's critical point in a controlled pore-size glass. Only a small critical temperature shift was observed for the confined fluid, which was attributed to both the weak fluid-pore interactions in this system and the relatively large pore sizes of the material used. The measured scaling exponent, for the confined fluid's critical temperature shift (from its bulk value) with average pore size, was once again shown to be in disagreement with the result predicted by finite-size scaling theory (Fisher and Nakanishi, 1981). Wong and Chan (1990) measured the pore coexistence curve of ^4He in a highly porous silica aerogel and found a narrow pore coexistence curve fully enclosed within the bulk fluid's coexistence curve; the critical temperature shift of the pore fluid was estimated to be about 31 mK, and the value of the critical exponent β was found to be 0.28 ± 0.05 K, which is in agreement with that for the *regular* three-dimensional Ising fluid. For N_2 in the same aerogel, this exponent's value was estimated to be 0.35 ± 0.05 K.

The preceding discussion is only illustrative of selected contributions as background for the study described here; a more extensive list of publications can be found in a recent review, by Pitard et al. (1996).

Phase Transitions in Quenched Random Pore Structures

In a porous system, the host material is made up of void space and complementary regions taken up by solid adsorbate material. In the void space one will, in general, find isolated molecules, those with nearest neighbors, and molecules adjacent to pore surfaces. Furthermore, pore-surface heterogeneities will generally be present, and all of these effects should be captured in any realistic model for analyzing the critical behavior of these systems. This, in our view, has yet to be achieved, and the main purpose of this article is to study an approach that advances these objectives. In the following section we describe the development of these ideas and proceed to illustrate their use for describing critical behavior and other thermodynamic properties in quenched, highly porous random systems.

The lattice gas we consider has a fixed number of matrix pore-blocked sites randomly assigned throughout the structure (see Figure 1). The remaining lattice sites are void spaces that may, or may not, be occupied by fluid particles. Nearset-neighbor fluid particles interact through a constant interaction energy, while solid matrix-fluid energetic interactions are represented by a probability function that represents the effect of binding site energy heterogeneity in the solid surface. We consider a simple cubic lattice in d dimensions and for each site define a quenched random variable ϵ_i, where ϵ_i can take on either the value 0 or 1. The value of 0, found with probability p, implies the existence of a solid matrix particle at that position in the lattice, while the value 1 designates a void space. In addition, at each void site we assign an annealed variable n_i, which can assume either the value 0, denoting the absence of a fluid particle, or 1, which represents the presence of a fluid particle; the variable n_i is the usual density variable associated with the lattice-gas partition function. The variables ϵ_i are assumed to be uncorrelated, an assumption justified for aerogels; the effects of correlations in the ϵ_i, relevant in a spinodally decomposed porous media like Vycor glass, will be dealt with in a subsequent article.

The Hamiltonian of this system is given by the equation:

$$-H_{LG} = 4\Im \sum_{\langle ij \rangle} \epsilon_i \epsilon_j n_i n_j + \Gamma \sum_{\langle ij \rangle} \left[\epsilon_i n_i (1-\epsilon_j) + \epsilon_j n_j (1-\epsilon_i) \right] + \mu \sum_i \epsilon_i n_i, \quad (1)$$

where $4\Im$ is the coupling constant between two adjacent fluid particles, Γ the coupling constant between a fluid and solid particle, and μ the chemical potential of the fluid. The summation in Eq. 1 (represented by the notation $\langle i,j \rangle$) is over all i,j pairs, but the effect of the ϵ_i, ϵ_j variables is to ensure that the first term in the Hamiltonian captures fluid–fluid interactions, the second term represents fluid–solid ones, while the third term is the standard field term for all fluid species in the matrix. By using the relationship connecting lattice-gas variables n_i, and Ising spin variable s_i, namely,

$$s_i \equiv 2n_i - 1, \quad (2)$$

we can easily transform Eq. 1 into its equivalent Ising Hamiltonian (up to a constant term) given by the equation:

$$-H_I = J \sum_{\langle ij \rangle} \epsilon_i \epsilon_j s_i s_j + K \sum_{\langle ij \rangle} \left[\epsilon_i s_i (1-\epsilon_j) + \epsilon_j s_j (1-\epsilon_i) \right] + B \sum_i \epsilon_i s_i + F(\epsilon_i, \ldots, \epsilon_j), \quad (3)$$

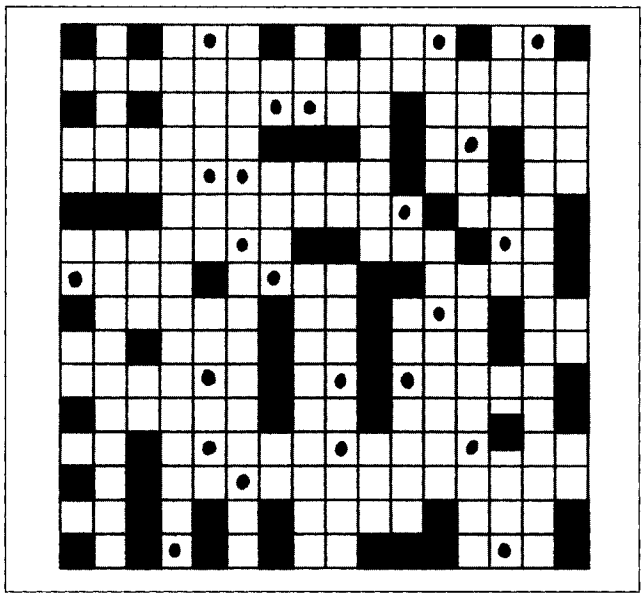

Figure 1. Matrix structure in a 2-D random lattice pore system.

where

$$F(\epsilon_i, \ldots, \epsilon_j) = \left[\frac{\mu}{2} + \frac{\Gamma z}{2}\right]\sum_i \epsilon_i - \Gamma \sum_{\langle ij \rangle} \epsilon_i \epsilon_j. \quad (4)$$

The variable z in Eq. 4 represents the lattice coordination number, while the function $F(\epsilon_i, \ldots, \epsilon_j)$ is dependent only upon the quenched variables ϵ_i and the parameters shown. At a specific value of the chemical potential it is constant for a given realization of the disorder in the system, and hence can be omitted from subsequent consideration. The relationships between the various parameters in the two Hamiltonians given in Eqs. 1 and 3 are given by the following equations:

$$J = \Im \quad (5)$$

$$K = \left(\frac{1}{2}\Gamma - \Im\right) \quad (6)$$

$$B = \left(\frac{\mu}{2} + \Im z\right). \quad (7)$$

Mean-field treatment: The confined lattice gas

The thermal average of molecular density at site i, which we define as $\langle n_i \rangle \equiv \rho$, is given by the rigorous statistical mechanical equation:

$$< n_i > \equiv \rho = \frac{\sum_{n_i=0,1} \cdots \sum_{n_k=0,1} n_i \exp[\beta H_{LG}]}{\sum_{n_i=0,1} \cdots \sum_{n_k=0,1} \exp[\beta H_{LG}]}, \quad (8)$$

where H_{LG} is given by Eq. 1 and $\beta \equiv 1/kT$. In the mean-field regime, however, we are able to simplify Eq. 8 considerably. Consider a site i surrounded by z sites, each of which may be pore-blocked, empty, or contain another molecule. The fundamental mean-field assumption is that molecules in any of these surrounding sites must be at their respective mean densities. If among these z neighboring sites, N of them are pore-blocked, then the probability of observing this configuration is given by the quantity Ω_N, defined as:

$$\Omega_N = \frac{z!}{(z-N)!N!}(1-p)^{z-N}p^N, \quad (9)$$

with $\Omega_{\text{total}} = \sum_{N=0}^{z} \Omega_N = 1$. Using this approach, Eq. 8 can be approximated in the mean-field situation by summing over the values $n_i = 0,1$ to get the the following equations,

$$< n_i > = \frac{1}{\Omega_{\text{total}}} \sum_{N=0}^{z} \frac{\Omega_N \exp[\beta(y_N + \mu)]}{\exp[\beta(y_N + \mu)] + 1} \quad (10)$$

or

$$< n_i > = \frac{1}{\Omega_{\text{total}}} \sum_{N=0}^{z} \times \frac{\Omega_N \exp[1/2\beta(y_N + \mu)]}{\exp[1/2\beta(y_N + \mu)] + \exp[-1/2\beta(y_N + \mu)]}, \quad (11)$$

which can be simplified to yield the equation:

$$< n_i > = \frac{1}{\Omega_{\text{total}}} \sum_{N=0}^{z} \times \frac{1}{2}\Omega_N[1 + \tanh 1/2\beta(y_N + \mu)], \quad (12)$$

where we have used a quantity y_N defined as

$$y_N \equiv 4\Im\langle n_i \rangle(z - N) + N\Gamma. \quad (13)$$

Substituting Eq. 9 in Eq. 12 yields the following result for the density of the confined fluid:

$$\rho = \frac{1}{2}\left\{1 + \sum_{N=0}^{z} \frac{z!}{(z-N)!N!}(1-p)^{z-N}p^N \cdot \tanh[1/2\beta(4\Im\rho(z-N) + N\Gamma + \mu)]\right\}, \quad (14)$$

which to first order in p yields the equation:

$$\boxed{(2\rho - 1) = (1 - zp)\tanh[\beta'(2z\rho + \mu'/2)] + zp\tanh[\beta'(2\rho(z-1) + 1/2\Gamma' + \mu'/2)],} \quad (15)$$

where we have made use of the following dimensionless quantities.

$$\beta' \equiv \beta \Im \tag{16}$$

$$\mu' \equiv \mu/\Im \tag{17}$$

$$\Gamma' \equiv \Gamma/\Im \tag{18}$$

$$T' \equiv 1/\beta' = kT/\Im. \tag{19}$$

Equation 15 is the central result of the first part of this article. It represents a new ***mean-field equation of state*** for a confined fluid in a highly porous quenched random structure. The corresponding equations for the Ising system are given in the Appendix.

Critical point for this model

The conditions for the critical point in this system are defined by the following two thermodynamic equations:

$$\left(\frac{\partial \mu'}{\partial \rho}\right)_{\beta_c'} = 0 \tag{20}$$

$$\left(\frac{\partial^2 \mu'}{\partial \rho^2}\right)_{\beta_c'} = 0. \tag{21}$$

To establish these derivatives we rewrite Eq. 15 more generally as

$$\rho = f(\rho, \beta', \mu'), \tag{22}$$

which together with Eqs. 20 and 21 give rise to the following equations at the critical point of this mean-field model:

$$\rho_c = f(\rho_c, \beta_c', \mu_c') \tag{23}$$

$$\left(\frac{\partial f}{\partial \rho}\right)_{\beta_c', \mu_c'} = 1 \tag{24}$$

$$\left(\frac{\partial^2 f}{\partial \rho^2}\right)_{\beta_c', \mu_c'} = 0. \tag{25}$$

Low p limit

The conditions given by Eqs. 23–25 provide three equations that can be solved for the critical values of T_c', μ_c', and ρ_c; however, these are implicit equations and for the low p limit we propose an analytic approximation for Eq. 15 by first defining perturbation functions χ and ϕ as follows:

$$\mu' - \mu'_{p=0} \equiv \chi(\beta', \Gamma')p \tag{26}$$

$$\rho - \rho_{p=0} \equiv \phi(\beta', \Gamma')p. \tag{27}$$

The functions χ and ϕ are as yet unknown, but solutions of Eq. 15 for $p = 0$ yield the values $\mu'_{p=0} = -2z$, $\rho_{p=0} = 1/2$. Using these equations in Eqs. 24 and 25, we find that,

$$2\phi(1 - \beta' z) = 2\beta'\chi + z \tanh(\beta'[1/2\Gamma' - 1]) \tag{28}$$

and

$$2z^2\beta'(z\phi + \chi) + (z-1)^2 z \tanh[\beta'(1/2\Gamma' - 1)] \operatorname{sech}^2[\beta'(1/2\Gamma' - 1)] = 0. \tag{29}$$

Solving both of these equations simultaneously for χ and ϕ, leads to the results:

$$\phi = \frac{1}{2z}\tanh[\beta'(1/2\Gamma' - 1)]\{z^2 - (z-1)^2 \operatorname{sech}^2[\beta'(1/2\Gamma' - 1)]\} \tag{30}$$

and

$$\chi = \frac{1}{2z\beta'}\tanh[\beta'(1/2\Gamma' - 1)] \cdot \left[z\beta'\{(z-1)^2\operatorname{sech}^2[\beta'(1/2\Gamma' - 1)] - z^2\} - (z-1)^2\operatorname{sech}^2[\beta'(1/2\Gamma' - 1)]\right]. \tag{31}$$

When Eqs. 30 and 31 are combined with Eqs. 15 and 24–27, *they yield the following results for the critical properties* ρ_c, T_c' *and* μ_c' *in the confined fluid to first order in* p:

$$\rho_c = \frac{1}{2} + \frac{1}{2}\tanh\left[\frac{\Gamma' - 2}{2z}\right]\left[z^2 - (z-1)^2\operatorname{sech}^2\left(\frac{\Gamma' - 2}{2z}\right)\right]p \tag{32}$$

$$T_c' = z\left[1 - p\{z - (z-1)\operatorname{sech}^2((\Gamma' - 2)/2z)\}\right] \tag{33}$$

$$\mu_c' = -2z^2\tanh\left[\frac{(\Gamma' - 2)}{2z}\right]p - 2z. \tag{34}$$

At the $p = 0$ limit, we can use Eqs. 32–34 to get the critical properties of the pure 3-D lattice gas model within a mean-field approximation. These results are given by the equations:

$$\rho_c(p = 0) = 1/2 \tag{35}$$

$$T_c'(p = 0) = z \tag{36}$$

$$\mu_c'(p = 0) = -2z \tag{37}$$

and conform with the established results for this system (Chandler, 1986).

At this point we make a few interesting observations based upon the preceding results:

- The mean-field model given in Eq. 15 shows that the fluid density (and hence its coexistence curve) will be a function of the relative strength of fluid–fluid and fluid–pore interactions; this is not the case with the van der Waal's-like mean-field model derived by Kierlik et al. (1998) for a similar Hamiltonian. In addition, it does not have the problem of being thermodynamically inconsistent (especially problematic for $d \leq 4$), similar to the mean-spherical integral equation model also described in that reference.
- For any given value of p, T_c' is a maximum for $\Gamma' = 2$. This implies that the critical temperature in the confined lattice-gas system is a *maximum* for a very specific strength of the fluid–solid coupling parameter, which we call $\Gamma'_{\max}$. This is true not only for the mean-field model described here but also in the exact lattice-gas system because of symmetry considerations.

Energy heterogeneity in the fluid–solid interaction

The results just derived can easily be extended to the situation where the fluid–solid interaction is given by a statistical distribution, that is, the surface is composed of sites with energetically heterogeneous binding energies. In this case, we assume that Γ' is given by a probability distribution, which we call $\eta(\Gamma')$. The mean-field equation is now modified so that the average of the righthand side in Eq. 33 is now taken. This leads to a critical temperature of the confined fluid given by the equation:

$$T_c' = z[1 - p\{z - (z-1)\gamma\}], \tag{38}$$

where γ is the average of $\text{sech}^2((\Gamma' - 2)/2z)$, defined by the integral:

$$\gamma = \int_{-\infty}^{\infty} \eta(\Gamma') \,\text{sech}^2\left(\frac{(\Gamma' - 2)}{2z}\right) d\Gamma'. \tag{39}$$

For a narrow distribution around some average energy Γ_0', we can derive a simple, useful expression for γ by Taylor expansion of $\text{sech}^2((\Gamma' - 2)/2z)$. This yields the result:

$$\gamma = \text{sech}^2\left(\frac{(\Gamma_0' - 2)}{2z}\right) + \frac{1}{2}\left[\frac{d^2\,\text{sech}^2\left(\frac{(\Gamma' - 2)}{2z}\right)}{d\Gamma'^2}\right]_{\Gamma' = \Gamma_0'} \int (\Gamma' - \Gamma_0')^2 \eta(\Gamma')\, d\Gamma'. \tag{40}$$

For a narrow Gaussian distribution, with standard deviation $\sigma \ll \Gamma_0'$, we find that

$$\gamma = \text{sech}^2\left(\frac{(\Gamma_0' - 2)}{2z}\right) + \frac{1}{2}\left[\frac{d^2\,\text{sech}^2\left(\frac{(\Gamma' - 2)}{2z}\right)}{d\Gamma'^2}\right]_{\Gamma' = \Gamma_0'} \sigma^2. \tag{41}$$

We now illustrate various qualitative and quantitative features of these results.

Numerical Calculations and Discussion

The calculations in this section of the article were done for a cubic 3-D lattice. In Figure 2 we show four adsorption isotherms at various values of p calculated at a dimensionless temperature $T' = 6$, with the value of the fluid–pore surface interaction parameter $\Gamma' = 4$. This temperature is the critical one for the zero p case as derived in Eq. 36, and the infinite slope of the $p = 0$ adsorption isotherm is evident at the critical chemical potential, which is equal to -12. As p increases, the system moves further away from criticality (into a supercritical temperature regime) and the slopes of the various isotherms become finite throughout the region shown.

The effect of porosity on the density enhancement of the adsorbed fluid, relative to the bulk fluid in thermodynamic equilibrium with it, can also be seen in the results given in

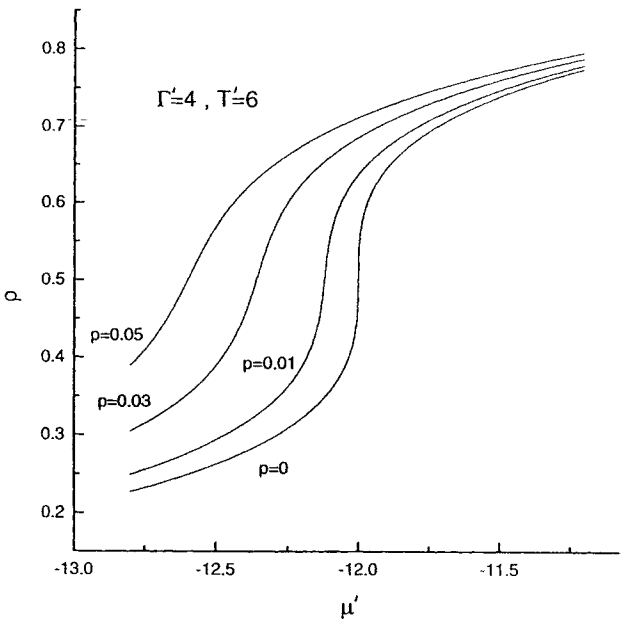

Figure 2. Adsorption isotherms at various values of p at the critical temperature of the pure lattice system, $p = 0$.

Figure 2. We look at the technologically interesting case where the fluid–pore interactions are attractive, that is, $\Gamma' > 0$. For a given value of both Γ' and temperature, the adsorbed fluid density is enhanced with increasing p. This enhancement is particularly pronounced in the lower pressure (chemical potential) region, a result that has been used in practical applications involving light gas storage in porous media. One would also expect that increasing the fluid–pore surface interaction parameter Γ', at a given temperature and value of p, should increase the magnitude of the adsorbed fluid's density. This is indeed the case, as shown in the results presented in Figure 3 for the situation $p = 0.03$ and a dimensionless temperature $T' = 6$.

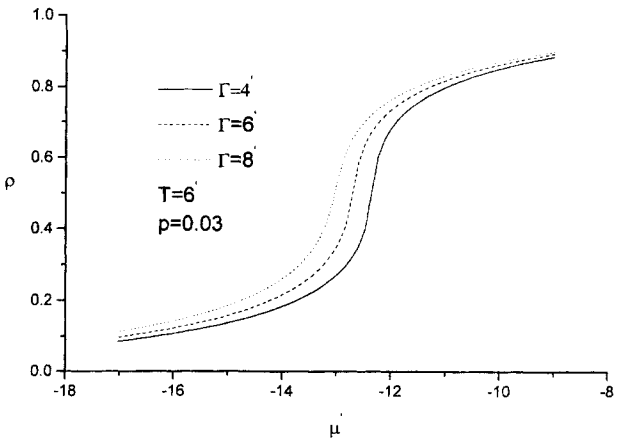

Figure 3. Supercritical adsorption isotherms at various values of the fluid–pore interaction parameter Γ' at the critical temperature of the pure lattice system, $p = 0$.

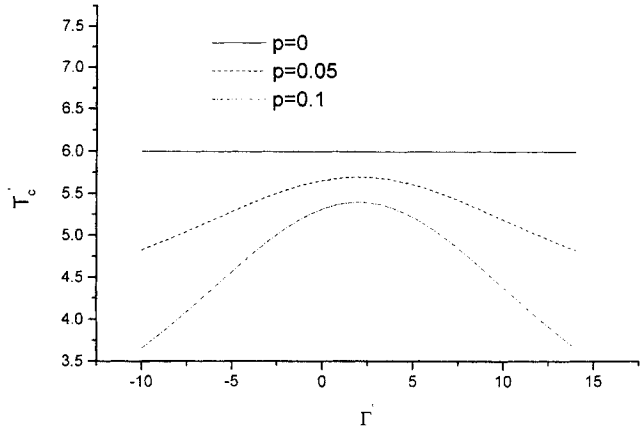

Figure 4. Mean-field predictions for the confined fluid's critical temperature as a function of both p and Γ'.

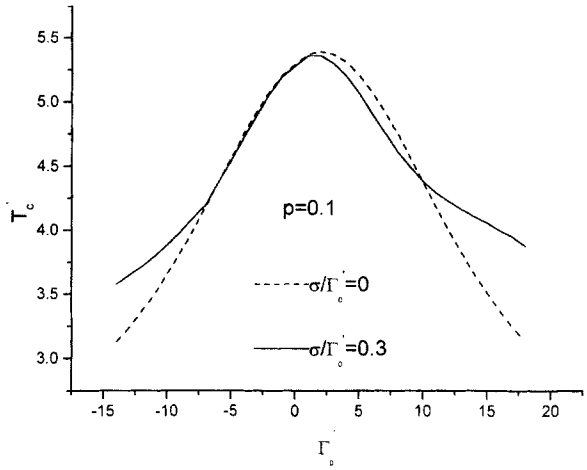

Figure 6. The effect of heterogeneity in the fluid–pore interaction energy on the critical temperature of a system, with $p = 0.1$.

The variation of the system's critical temperature with the fluid–pore surface interaction parameter Γ', at various values of p, is presented in Figure 4. We observe that the critical temperature decreases with increasing values of p, a result that follows mathematically from Eq. 33. As discussed earlier, the T_c' function must be symmetric about Γ'_{max} in any exact solution for this system for all values of p. Here we observe that the mean-field model preserves this symmetry property, with the critical temperature displaying a maximum at a value of Γ' equal to 2 *for all p*. This result implies the existence of two random pore systems with *identical critical temperatures and porosities but different values of* ρ_c and μ_c'. These two systems possess values of Γ' equidistant from Γ'_{max}; the different behavior of these two systems is illustrated in Figure 5, where we used the two values of Γ' equidistant from Γ'_{max} (that is, 0 and 4, for the case $p = 0.1$) to calculate the ρ vs. μ' isotherms at a temperature slightly above the critical one. The results shown in Figure 5 confirm the quite different behavior of these two systems despite their having identical porosities and critical temperatures. The ability of the system with a higher value of Γ' to induce the transition from the low- to a high-density state for the confined fluid at a much lower chemical potential (pressure) is clear.

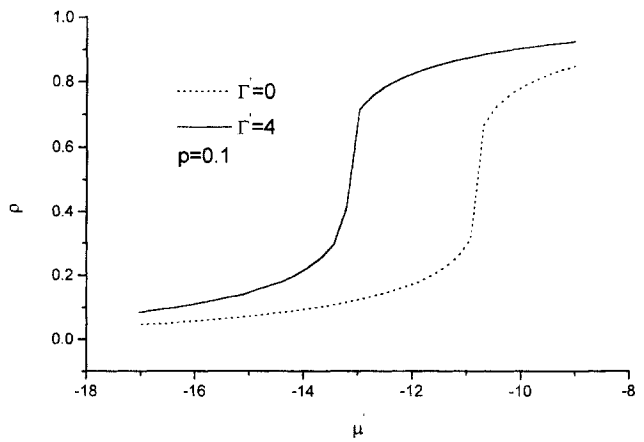

Figure 5. Supercritical adsorption isotherms at $p = 0.1$ for two symmetric porous systems, possessing values of Γ' equidistant from Γ'_{max}.

In any real material the fluid–pore energy interaction parameter Γ' is likely to be heterogeneous, a feature that we incorporated into our theoretical formulation of the mean-field model. For the results shown in Figure 6 for $p = 0.1$, the distribution of the energy heterogeneity was assumed to follow a Gaussian form with $\sigma/\Gamma'_0 = 0.3$. The effect of this heterogeneity on the critical temperature of the system is to widen the distribution of the $T_c'(\Gamma')$ function about Γ'_{max}. For a range of values of Γ'_0 in the vicinity of Γ'_{max}, the value of the critical temperature in the energetically heterogeneous system is smaller than in the system with a uniform distribution of adsorption binding energies, a result that is qualitatively consistent with prior simulation results (Gac et al., 1996); outside of this range the converse appears to be true.

The two-phase region of the confined fluid is a property of fundamental interest in dealing with porous materials. This can be found with the mean-field model using the Maxwell construction and ρ vs. μ' isotherms. In Figure 7 we show how this can be done using an example of a subcritical isotherm with $T' = 4$ in a system with $p = 0.1$ and $\Gamma' = 8$. The chemical potential that gives rise to equal areas for each of the van der Waals loops (shown as areas A and B in Figure 7) reflects the point of phase coexistence in the medium. Locating this value of μ' allows one to calculate the densities of the coexisting phases at the given conditions. This type of construction was done at several temperatures and from these results the phase boundary of the confined fluid was developed, with the results given in Figure 8. This coexistence boundary is asymmetric, as would be expected in random systems of this sort.

The discussion to this point has centered around specific qualitative predictions of the model. We now investigate its quantitative accuracy for predicting adsorption behavior in these types of systems. Ideally this issue requires exact solutions for the system free energy (and related quantities) to be available for comparative purposes. To our best knowledge,

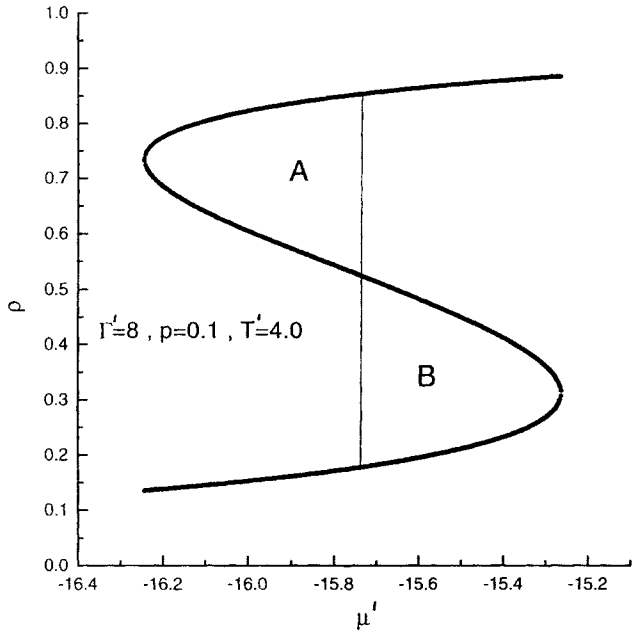

Figure 7. Maxwell construction for a subcritical isotherm.

such results are not currently available, and as a consequence we resorted to computer simulation to provide a set of benchmarks to be used for this purpose; some of the results from this effort are now presented. The simulations were performed using grand canonical Monte Carlo 3-D simulation of confined lattice gas with periodic boundary conditions. The lattice contained solid impurities (pore-blocked sites) distributed throughout the medium. These solid sites were distributed in the lattice randomly such that each site

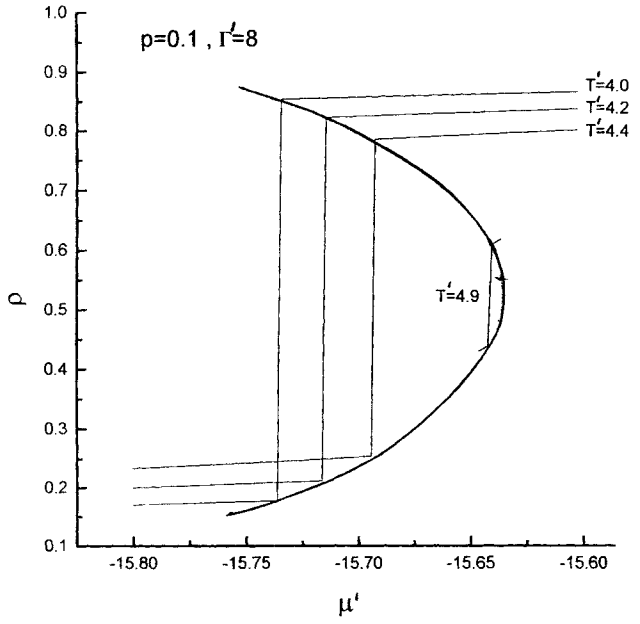

Figure 8. Phase coexistence boundary for the confined fluid at $p = 0.1$.

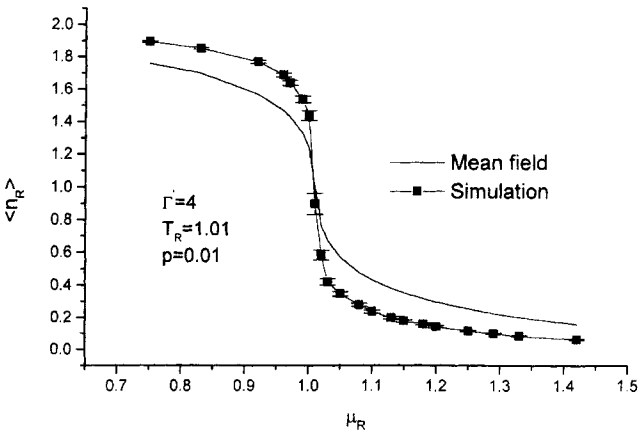

Figure 9. Simulation data vs. mean-field predictions for the adsorption isotherm of the confined fluid at $p = 0.01$.

had a probability p of being a solid particle. The interactions between the fluid and solid (pore) particles were governed by an interaction potential analogous to Γ' in the mean-field model. The simulations were performed on a cubic lattice of side 24 units. On average the simulations for each run used approximately $3E05$ MCS to reach equilibrium (Gac et al., 1996), with a preequilibration process involving approximately $1.0E05$ Monte Carlo steps per site (MCS). The simulation data were averaged over at least five different realizations of the media to reduce dependence of the results on any particular single realization. Each of the plots of the simulation data show points averaged over all the realizations used. The error bars for each simulation data represent the number density fluctuation of the fluid in the lattice at the given conditions.

Some comparisons between the mean-field and simulation results are given in Figures 9–11. Figure 9 shows a comparison of adsorption isotherms of both the mean-field model and simulation results in a highly porous system ($p = 0.01$) at a slightly supercritical temperature corresponding to a reduced temperature of 1.01. *The reducing parameters for all the thermodynamic properties in these comparisons were the corresponding critical values in the respective pure systems (that is, $p = 0$).* These are known exactly for the lattice gas (Ferrenberg and Landau, 1991), and were used here for the simulation results, while those for the mean-field model were found from the results of this work, that is, Eqs. 35–37. The shapes of the isotherms for both sets of results in Figure 9 are quite similar. The mean-field density predictions are smaller than the simulation results at the higher densities, with the reverse being true at lower densities. The proximity of the system to criticality is evident in the simulation results, with the steep part of the isotherm occurring in the neighborhood $\mu_R = 1.0$. This is less evident in the mean-field results, as would be expected for this model, since critical fluctuations are neglected; these are considered crucial for accurately describing behavior near the critical point. Figure 10 contains results for another system at the same reduced temperature and value of Γ', but higher porosity ($p = 0.05$). At this higher porosity but same temperature the system is further removed from

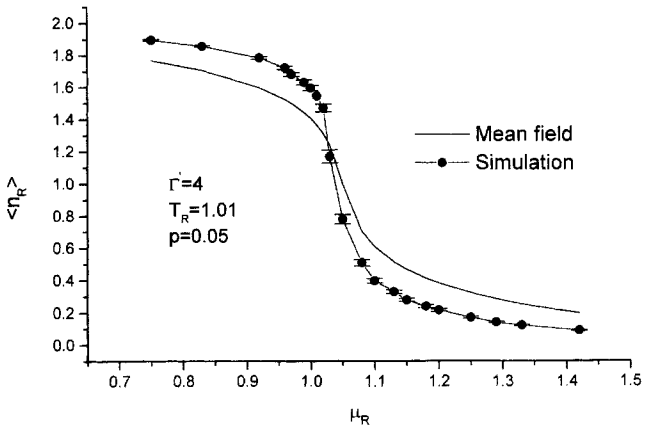

Figure 10. Simulation data vs. mean-field predictions for the adsorption isotherm of the confined fluid at $p = 0.05$.

criticality. As a result the effects of fluctuations in the fluid are diminished, which should lead to an improvement in the agreement between the mean-field and simulation results, a result borne out by the results presented in Figure 10. However, a more convincing demonstration of the increasing accuracy of the mean-field model at conditions increasingly remote from the critical point is given in Figure 11. The results presented there are for a system with $p = 0.1$, $\Gamma' = 8$ at two different reduced temperatures corresponding to $T_R = 1.00$ and $T_R = 1.33$, respectively. The average absolute deviation between the mean-field model and simulation results at the lower (closer to critical) temperature is about 10.3%, while at the higher temperature this figure is 7.4%. These results are, in our view, encouraging for a completely analytic theory in a complex fluid system of this sort. More detailed numerical comparisons at other temperatures and porosities for the system are given in Tables 1 and 2. In general there is quite good agreement between the mean-field model and simulation results, with the best results at higher densities and increasing p-consistent with the results presented earlier.

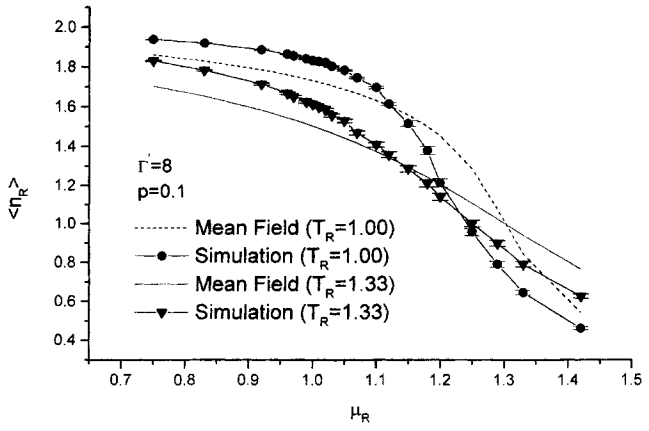

Figure 11. Simulation data vs. mean-field predictions for the adsorption isotherm of the confined fluid at various supercritical temperatures.

Table 1. Reduced Densities Predicted by Mean Field and Simulation Results at Various Reduced Temperatures with $p = 0.1$ and $\Gamma' = 0.8$*

μ_R	Simulation $T/T_c = 1.06$	Mean Field $T/T_c = 1.06$	Simulation $T/T_c = 1.11$	Mean Field $T/T_c = 1.11$
0.75	1.921	1.834	1.908	1.811
0.83	1.895	1.8	1.878	1.773
0.92	1.856	1.749	1.834	1.718
0.96	1.831	1.721	1.805	1.687
0.97	1.818	1.713	1.791	1.679
0.99	1.800	1.697	1.771	1.661
1	1.791	1.688	1.761	1.652
1.01	1.783	1.679	1.753	1.642
1.02	1.778	1.67	1.746	1.632
1.03	1.754	1.66	1.72	1.622
1.05	1.732	1.639	1.697	1.599
1.07	1.685	1.616	1.645	1.575
1.1	1.63	1.577	1.588	1.533
1.12	1.545	1.548	1.504	1.502
1.15	1.453	1.496	1.417	1.449
1.18	1.333	1.434	1.306	1.386
1.2	1.194	1.385	1.183	1.337
1.25	0.969	1.225	0.976	1.188
1.29	0.818	1.054	0.834	1.043
1.33	0.682	0.876	0.703	0.896
1.42	0.499	0.599	0.521	0.64

*The average absolute deviations between the simulation and mean field data are 9.47% at $T/T_c = 1.06$ and 9.17% at $T/T_c = 1.11$.

For the final set of results we focused on how the mean-field model is to be used with experimental data. For this purpose we used experimental adsorption data for methane in a silica aerogel at 308 K taken from Masukawa and Kobayashi (1968). Such data are usually represented as pressure (chemical potential) -density adsorption isotherms. The mean-field equation of state given earlier in the article (Eq.

Table 2. Reduced Densities Predicted by Mean Field and Simulation Results at Various Porosities at a Reduced Temperature of 1.33

μ_R	Simulation $p = 0.01$	Mean Field $p = 0.01$	Simulation $p = 0.05$	Mean Field $p = 0.05$
0.75	1.722	1.53	1.734	1.55
0.83	1.616	1.42	1.64	1.453
0.92	1.424	1.244	1.483	1.305
0.96	1.264	1.142	1.36	1.222
0.97	1.183	1.115	1.3	1.199
0.99	1.092	1.058	1.234	1.152
1	1.048	1.029	1.198	1.127
1.01	1	1	1.161	1.102
1.02	0.952	0.97	1.122	1.077
1.03	0.862	0.941	1.044	1.051
1.05	0.776	0.884	0.965	1
1.07	0.669	0.83	0.847	0.547
1.1	0.581	0.756	0.748	0.872
1.12	0.509	0.711	0.661	0.824
1.15	0.452	0.65	0.585	0.757
1.18	0.403	0.597	0.522	0.697
1.2	0.363	0.565	0.471	0.66
1.25	0.3	0.496	0.388	0.58
1.29	0.26	0.449	0.333	0.523
1.33	0.226	0.409	0.29	0.477
1.42	0.176	0.335	0.224	0.39

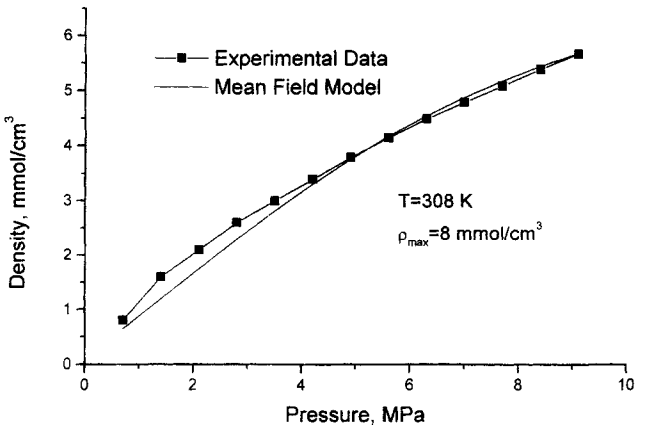

Figure 12. Mean-field model predictions when fitted to experimental adsorption data for methane in silica aerogel at 308 K.

Masukawa and Kobayashi, 1968: optimal value of $\Im = 26.7 \times 10^{-23}$ J; $\Gamma' = 11.8$ in units of $\Im$.

15) provides a way of a calculating the variation of density with chemical potential along the experimental isotherm, given assumed values of the model parameters Γ' and $\Im$ at a given value of porosity, which is often known from independent measurements. Integration of this function provides the pressure change in the system between any two chosen states 1 and 2 using the following thermodynamic identity:

$$\Delta P_{1-2} = \int_{\mu_1'}^{\mu_2'} \rho(\Gamma', \Im, \beta')\, d\mu'. \tag{42}$$

One can repeat this series of calculations in an attempt to optimize the values of Γ' and $\Im$, by which we mean establishing their values that provide the best match between the model predicted pressure change given by Eq. 42 with that shown in the data. These results are shown in Figure 12 for $p = 0.05$ and illustrate very good agreement between the model and these data, especially at the higher pressures where this agreement is often to within 1%. The average absolute deviation between the model and data over the entire data set is 6.9%.

Conclusions

In this first of a series of article we have presented a new mean-field equation of state for modeling the thermodynamic behavior of a fluid confined in a highly porous, quenched random structure. The Hamiltonian for the system includes terms representing both fluid–fluid and fluid–pore interactions, and the effects of confinement are explicitly addressed, since a fluid molecule can find itself with either fluid and/or pore-surface neighbors or surrounded by a void. In addition to representing uniform fluid–pore surface binding energies the model was also developed to accommodate the situation where adsorption binding interactions are assumed to be heterogeneous following some prescribed probability density function.

Given these assumptions, novel results for the fluid's critical properties in the confined system were derived for the low p limit. These equations show the dependence of the critical temperature, density, and chemical potential on porosity and the fluid–pore interaction energy Γ'. The model predicts a decreasing value of T_c' with increasing porosity, and, for all values of p, it shows a maximum in this temperature at a specific value of the pore–fluid interaction parameter, which we designated as Γ'_{max}. The $T_c'(\Gamma')$ function for the mean-field model retains the necessary symmetry around Γ'_{max}, implying the existence of two independent fluid–pore systems with identical values of p and T_c', but different values of ρ_c and μ_c'. The effect of heterogeneity in the fluid–pore surface interaction energy, at a specific p, was shown to substantially diminish the value of the critical temperature T_c'. The model also predicts phase coexistence of the confined fluid with an asymmetric coexistence boundary around the critical point, as would be theoretically expected in a random system of this sort.

In various comparisons with adsorption isotherms generated by GCMC computer simulations, the mean-field model showed quite good agreement with the simulation data. This agreement improved, as expected, at conditions farther from the critical point. The incorporation of the effects of fluctuations in the model should improve the quantitative accuracy of the model, especially in the critical region. Since many engineering applications require knowledge of the fluid system in the near-critical region, this is an important area for further research that we are currently pursuing.

Acknowledgment

The authors acknowledge the National Science Foundation, which provided financial support for this work through Grant CTS-9706805.

Notation

B = external field in Ising model
f = equation-of-state function
F = function of random variables
H = Hamiltonian function
J = nearest-neighbor coupling parameter in Ising model
k = Boltzmann's constant
K = spin–solid coupling parameter in Ising model
m = magnetization
n = molecular density in lattice gas
p = density of particles in porous matrix
P = pressure
s = spin variable in Ising model
T = temperature
y = function in Hamiltonian
z = lattice coordination number

Greek letters

$\beta = 1/kT$
ϵ = random variable
μ = chemical potential
χ = perturbation function
ϕ = perturbation function
η = energy probability function
γ = average in energy probability function
Γ = fluid–solid coupling parameter in lattice gas
σ = standard deviation of energy distribution
$\Im$ = nearest-neighbor coupling parameter in lattice gas
ρ = fluid density
Ω = configuration degeneracy

Subscripts and superscripts

0 = mean value
i = component I
c = critical property
I = Ising model property
LG = lattice-gas property
N = number of pore-blocked sites
$'$ = dimensionless property

Literature Cited

Afrane, G., and E. H. Chimowitz, "Experimental Investigation of a New Supercritical Fluid-Inorganic Membrane Separation Process," *J. Membr. Sci.*, **116**, 293 (1996).

Ayappa, K. G., C. R. Kamala, and T. A. Abinandanan, "Mean Field Lattice Model for Adsorption Isotherms in Zeolite NaA," *J. Chem. Phys.*, **110**, 8714 (1999).

Blumel, S., and G. H. Findenegg, "Critical Adsorption of a Pure Fluid on a Graphite Substrate," *Phys. Rev. Lett.*, **54**, 447 (1985).

Chandler, D., *Introduction to Modern Statistical Mechanics*, Oxford Univ. Press, New York (1986).

Cracknell, R. F., P. Gordon, and K. E. Gubbins, "Influence of Pore Geometry on the Design of Microporous Materials for Methane Storage," *J. Phys. Chem.*, **97**, 494 (1993).

DeGennes, P. G., "RFIM as Model for Porous Media," *J. Chem. Phys.*, **88**, 6649 (1984).

Evans, R., "Fluid Adsorbed in Narrow Pores: Phase Equilibria and Structure," *J. Phys. Condensed Matter*, **2**, 8989 (1990).

Evans, R., U. M. B. Marconi, and P. Tarazona, "Capillary Condensation and Adsorption in Cylindrical and Slit-Like Pores," *J. Chem. Soc. Faraday Trans.*, **82**, 1763 (1986).

Fanti, L. A., E. D. Glandt, and W. G. Madden, "Fluids in Equilibrium with Disordered Media," *J. Chem. Phys.*, **93**, 5945 (1990).

Ferrenberg, A. M., and D. P. Landau, "Critical Behavior of the Three-Dimensional Ising Model: A High Resolution Monte Carlo Study," *Phys. Rev. B*, **44**, 5081 (1991).

Findenegg, G. H., and R. Loring, "Fluid Adsorption up to the Critical Point: Experimental Study of a Wetting Fluid/Solid Interface," *J. Chem. Phys.*, **81**, 3270 (1984).

Findenegg, G. H., and J. Specovius, "Study of a Fluid/Solid Interface Over a Wide Density Range Including the Critical Region: 2. Spreading Pressure and Enthalpy of Adsorption of Ethylene/Graphite," *Ber. Bunsenges. Phys. Chem.*, **84**, 696 (1980).

Fisher, M. E., and H. Nakanishi, "Scaling Theory for the Criticality of Fluids Between Plates," *J. Chem. Phys.*, **75**, 5857 (1981).

Fishman, S., and A. Aharony, "Random Field Effects in Disordered Anisotropic Antiferromagnets," *J. Phys. C*, **12**, L729 (1979).

Gac, W., M. Kruk, A. Patrykiejew, and S. Sokolowski, "Effects of Random Quenched Impurities on Layering Transitions: A Monte Carlo Study," *Langmuir*, **12**, 159 (1996).

Goh, M. C., W. I. Goldburg, and C. M. Knobler, "Phase Separation of a Binary Liquid Mixture in a Porous Medium," *Phys. Rev. Lett.*, **58**, 1008 (1987).

Imry, Y., and S. K. Ma, "Random Field Instability of the Ordered State of Continuous Symmetry," *Phys. Rev. Lett.*, **35**, 1399 (1975).

Jing, S., K. E. Gubbins, and P. B. Balbuena, "Theory of Adsorption of Trace Components," *J. Phys. Chem.*, **98**, 2403 (1994).

Kaminsky, R. D., and P. A. Monson, "The Influence of Adsorbent Microstructure upon Adsorption Equilibrium: Investigation of a Model System," *J. Chem. Phys.*, **95**, 2936 (1991).

Kaminsky, R. D., and P. A. Monson, "A Simple Mean Field Theory of Adsorption in Disordered Porous Materials," *Chem. Eng. Sci.*, **49**, 2967 (1994).

Kierlik, E., M. L. Rosinberg, G. Tarjus, and E. Pitard, "Mean-Spherical Approximation for a Lattice Model of a Fluid in a Disordered Matrix," *Mol. Phys.*, **95**, 341 (1998).

MacFarland, T., G. T. Barkema, and J. F. Marko, "Equilibrium Phase Transitions in a Porous Medium," *Phys. Rev. B*, **53**, 148 (1996).

Madden, W. G., and E. D. Glandt, "Distribution Functions in Random Media," *J. Stat. Phys.*, **51**, 537 (1988).

Maritan, A., M. R. Swift, M. Cieplak, M. H. W. Chan, M. W. Cole, and J. R. Banavar, "Ordering and Phase Transitions in Random Field Ising Systems," *Phys. Rev. Lett.*, **67**, 1821 (1991).

Masukawa, S., and R. Kobayashi, "Methane-Ethane-Silica Gel at High Pressures and Ambient Temperatures," *J. Chem. Eng. Data*, **13**, 197 (1968).

Patrykiejew, A., "Monte Carlo Study of Adsorption on Heterogeneous Surfaces: Finite Size and Boundary Effects in Localized Monolayers," *Langmuir*, **9**, 2562 (1993).

Pitard, E., M. L. Rosinberg, and G. Tarjus, "Thermodynamics of Fluids in Disordered Porous Materials," *Mol. Simulation*, **17**, 399 (1996).

Plischke, M., and B. Bergersen, *Equilibrium Statistical Physics*, World Scientific, Singapore (1994).

Rangarajan, R., and C. T. Lira, "Production of Aerogels," *J. Supercrit. Fluids*, **4**, 1 (1991).

Specovius, J., and G. H. Findenegg, "Physical Adsorption of Gases at High Pressures: Argon and Methane onto Graphitized Carbon Black," *Ber. Bunsenges. Phys. Chem.*, **82**, 174 (1978).

Specovius, J., and G. H. Findenegg, "Study of a Fluid/Solid Interface over a Wide Density Range Including the Critical Region 1. Surface Excess of Ethylene/Graphite," *Ber. Bunsenges. Phys. Chem.*, **84**, 690 (1980).

Tan, Z., and K. E. Gubbins, "Adsorption in Carbon Micropores at Supercritical Temperatures," *J. Phys. Chem.*, **94**, 6061 (1990).

Tapia-Corzo, C., V. Kumaran, and E. H. Chimowitz, "Experimental Study of Retrograde Adsorption in Supercritical Fluids," *J. Supercritical Fluids*, **17**, 25 (2000).

Tarazona, P., "Free Energy Density Functional Theory for Hard Spheres," *Phys. Rev. A*, **31**, 2672 (1985).

Thommes, M., and G. H. Findenegg, "Critical Depletion of a Pure Fluid in Controlled-Pore Glass. Experimental Results and Grand Canonical Ensemble Monte Carlo Simulation," *Langmuir*, **11**, 2137 (1995).

Thommes, M., and G. H. Findenegg, "Pore Condensation and Critical Point Shift of a Confined Fluid in Controlled Pore Glass," *Langmuir*, **10**, 4270 (1994).

VonBehren, J., E. H. Chimowitz, and P. M. Fauchet, "Critical Behavior and the Processing of Nanoscale Porous Materials," *Adv. Mat.*, **9**, 921 (1997).

Wang, Q., and J. K. Johnson, "Computer Simulations of Hydrogen Adsorption on Graphite Nanofibers," *J. Phys. Chem. B*, **103**, 1 (1999a).

Wang, Q., and J. K. Johnson, "Molecular Simulation of Hydrogen Adsorption in Single-Walled Carbon Nanotubes and Idealized Carbon Slit Pores," *J. Chem. Phys.*, **110**, 577 (1999b).

Wong, A. P. Y., and M. H. W. Chan, "Liquid-Vapor Critical Point of He in Aerogel," *Phys. Rev. Lett.*, **65**, 2567 (1990).

Wong, A. P. Y., S. B. Kim, W. I. Goldburg, and M. W. H. Chan, "Phase Separation, Density Fluctuations and Critical Dynamics of Nitrogen in Aerogel," *Phys. Rev. Lett.*, **70**, 954 (1993).

Appendix: Mean-Field Model for the Confined Ising System at Low p Limit

We now consider a spin at a particular site i that does not have a solid particle at that position. If the time average of the magnetization at this site is designated as $\langle m_i \rangle$, then the local mean-field equation for the magnetization at this site can be written as

$$\langle m_i \rangle = \tanh\left[\beta \sum_{\langle j \rangle_i} \left(\epsilon_j J m_j + \left(1 - \epsilon_j\right) K + B \right) \right], \quad \text{(A1)}$$

where the $\langle j \rangle_i$ term in Eq. 43 denotes a sum over neighboring sites of i, and B is a uniform external field with magnitude related to both variables μ, $\Im$ of the lattice gas given by Eq. 7.

If we assume that for every site $\langle m_i \rangle \equiv m$, then averaging over all possible neighborhood configurations of i, we obtain

$$m = \sum_{n=0}^{z} \left\{ \begin{matrix} z \\ n \end{matrix} \right\} (1-p)^{z-n} p^n \tanh\left[\beta(J(z-n)m + nK + B) \right], \tag{A2}$$

where

$$\left\{ \begin{matrix} z \\ n \end{matrix} \right\} \equiv \frac{z!}{(z-n)!n!}.$$

This equation bears a resemblance to the usual mean-field result for an (unconfined) Ising system but contains additional variables like p and K that account for the effects of confinement in the porous medium. Since we are interested in the low p limit, we take the first order in p terms in this equation, which then becomes

$$m = (1-zp)\tanh\left[\beta(Jzm + B) \right] + zp \tanh\left[\beta(J(z-1)m + K + B) \right], \tag{A3}$$

in which case Eq. 43 becomes

$$m = (1-zp)\tanh\left[\beta'(zm + B') \right] + zp \tanh\left[\beta'((z-1)m + K' + B') \right], \tag{A4}$$

where we have defined the quantities

$$\begin{aligned} \beta' &= \beta J \\ K' &= K/J \\ B' &= B/J. \end{aligned} \tag{A5}$$

For the Ising model results given here we see that for $K = 0$, $T_c = z(1-p)$, which is the known result for the SD Ising model in the mean-field regime (Plischke and Bergersen, 1994). Also for a cubic lattice, in the limit $p \to 0$, $T_c = 6$, and for any value of K (both positive and negative), the critical temperature for finite p is always predicted to be less than the zero p case. We emphasize that the Ising model here is different from both those of the standard RFIM and site-dilute Ising model (SDIM) Hamiltonians usually considered in the literature.

Manuscript received Sept. 29, 1999, and revision received July 10, 2000.